Characterization of an ultraviolet and a vacuum-ultraviolet irradiance meter with synchrotron radiation

Ping-Shine Shaw, Rajeev Gupta, and Keith R. Lykke

We have constructed and characterized a simple probe that is suitable for accurate measurements of irradiance in the UV to the vacuum UV spectral range. The irradiance meter consists of a PtSi detector located behind a 5-mm-diameter aperture. The probe was characterized at various wavelengths ranging from 130 to 320 nm by use of continuously tunable synchrotron radiation from the Synchrotron Ultraviolet Radiation Facility III. We determined the irradiance responsivity by scanning a small monochromatic beam over the active area of the irradiance meter and measuring its response on a grid with regular spacing. The angular response was also determined and shown to be suitable for applications such as photolithography. In addition, we studied the radiation damage using a 157-nm excimer laser and found that the irradiance meter can endure more than 100 J/cm^2 of 157-nm radiation before a noticeable change occurs in its responsivity. Many industrial applications such as UV curing, photolithography, or semiconductor chip fabrication that require accurate measurement of the irradiance would benefit from having such a stable, accurate UV irradiance meter.

OCIS codes: 120.5630, 120.0280, 040.6070, 040.7190.

1. Introduction

Irradiance meters are well developed and widely used over the spectral range from the infrared to the UV. In the UV, considerable effort has been devoted to irradiance meter development and calibration due to a wide range of applications for which accurate UV measurements are required.[1] Recently, industrial applications, such as UV curing and semiconductor photolithography, have pushed the measurement needs into the vacuum-ultraviolet (VUV) region. The UV and VUV regions pose significant complexities[2] in the development of irradiance meters compared with their counterparts in the near UV to the infrared because detectors are susceptible to radiation damage; there are only a few optical components (filters, diffusers, etc.) available; and calibration techniques do not have the necessary accuracy. To improve the accuracy of UV and VUV irradiance measurements, we have designed, constructed, characterized, and calibrated an irradiance meter based on a recently developed UV solid-state photodiode. The instrument was calibrated at a number of UV wavelengths including several excimer-laser wavelengths, e.g., 157 and 193 nm, that are important for the semiconductor and UV-curing industries.

The characterization and calibration of this new irradiance meter were performed at a detector-based radiometry beamline by use of continuously tunable synchrotron radiation from the Synchrotron Ultraviolet Radiation Facility (SURF)[3] at the National Institute of Standards and Technology (NIST). This beamline[4,5] was designed primarily to calibrate the power response of UV detectors from 130 to 320 nm. Typically, the calibration of irradiance responsivity requires radiation sources with uniform power distribution across the entrance area of the irradiance meter. For example, NIST's Spectral Irradiance and Radiance Responsivity Calibrations with Uniform Sources (SIRCUS) Facility[6] uses lasers with an integrating sphere to produce a uniform irradiant distribution at a reference plane. Irradiance meters are placed in the uniform field and the responses from the meter under test are measured. The wavelength range of SIRCUS, however, is ultimately limited by the laser system to wavelengths longer than 200 nm. Furthermore, the throughput of the integrating sphere decreases dramatically into the UV region, which results in a much less uniform radiation output that could affect the accuracy of calibration.

An alternative technique for irradiance responsivity calibration is to use a monochromatic and collimated beam to raster scan the entire active area of

The authors are with the Optical Technology Division, National Institute of Standards and Technology, Gaithersburg, Maryland 20899. P.-S. Shaw's e-mail address is shaw@nist.gov.

Received 16 April 2002; revised manuscript received 26 August 2002.

the irradiance meter. This technique for irradiance calibration was demonstrated previously for near-UV and visible radiation.[7–9] Utilizing the UV and VUV radiation available at the SURF, we were able to use this calibration technique to calibrate irradiance meters at wavelengths as short as 130 nm.

In addition to the irradiance responsivity calibration, we also studied the effects of UV exposure on the responsivity of the irradiance meter and its angular response to the incident radiation. Deviation from an ideal cosine response usually occurs at large incident angles, thus limiting the useful viewing angle of the irradiance meter to the incident radiation.[2]

The important issue peculiar to UV and VUV studies involves the stability of the detectors under irradiation. The changes in the response of an irradiance meter affect the measurement accuracy. Radiation damage resistance must be studied to determine the frequency of recalibration of the specific detector required to achieve the necessary accuracy. The more resistant a detector is to damage from UV radiation, the more reliable it is in radiation measurements. For our design of the UV irradiance meter, we used a PtSi-windowed silicon photodiode with much improved radiation hardness as the detector. We tested this detector to assess radiation resistance quantitatively by using a 157-nm excimer laser. The response of the detector was measured as a function of the total amount of irradiation.

2. Irradiance Meter and Characterization Facility

The irradiance meter was constructed with an UV photodiode from International Radiation Detectors, Inc.[10] This photodiode is a silicon photodiode with a thin PtSi front window instead of the traditional SiO_2 front window to increase its hardness against UV radiation.[11] The photodiode has an active area of 10 mm $\times$ 10 mm. An aperture with a diameter of 5 mm was attached immediately to the front of the photodiode. The close proximity of the aperture and the detector surface reduces the effect of incident radiation multireflecting between the detector surface and the aperture.

The facility used to calibrate and characterize the irradiance meter is the cryogenic radiometry beamline at SURF III.[4] The beamline consists of a 2-m monochromator followed by refocusing optics, a detector test chamber, and a liquid-helium-cooled cryogenic radiometer. The cryogenic radiometer serves as the primary standard for detector calibrations. The overall relative uncertainty achieved is less than 0.5% for spectral power responsivity calibrations in the range from 130 to 320 nm. A detailed description of the beamline components and uncertainty analysis can be found elsewhere.[4]

Inside the detector chamber, the test detector is mounted on an x-y motorized stage and can be accurately positioned and scanned in the plane perpendicular to the incident beam. The test detector can also be rotated to change both the incident angle and the polarization state of the incident beam since synchrotron radiation is highly polarized. In addition, the test detector can be irradiated with a 157-nm laser beam for damage studies. The laser beam entered the chamber through a MgF_2 window port on one side of the chamber.

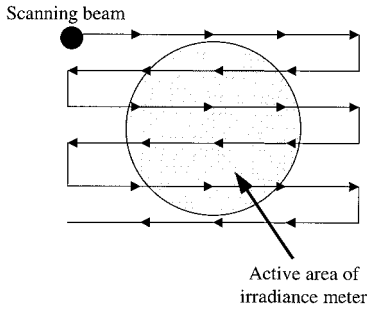

Fig. 1. Beam scanning technique for irradiance responsivity calibration.

3. Methodology of Irradiance Responsivity Calibration

The irradiance responsivity of an irradiance meter, R (A/W cm^2), is defined as

$$R \equiv \frac{i}{E} = \iint_A s(x, y)\mathrm{d}x\mathrm{d}y, \tag{1}$$

where i (A) is the current from the irradiance meter, E (W/cm^2) is the irradiance, and $s(x, y)$ (A/W) is the power responsivity of the detector at location (x, y) of the detector surface. The integral is over the area of the irradiance meter's aperture A since $s(x, y)$ vanishes outside the aperture area. For irradiance meters with a uniform power responsivity, s_0, across its active area, the irradiance responsivity of Eq. (1) reduces to the power responsivity s_0 multiplied by the area of its aperture.

To measure R for more general cases, we used a probe beam to raster across the entire detector surface (see Fig. 1) while we measured the response of the detector. Assuming that the probe beam has the same relative intensity distribution or a normalized flux density $\Phi_n(x - x', y - y')$, and the total power of probe beam $P(x', y')$ relative to reference point (x', y'), the function $\Phi_n(x - x', y - y')$ is normalized such that

$$\iint_S \Phi_n(x - x', y - y')\mathrm{d}x\mathrm{d}y = 1, \tag{2}$$

where the area of integral S is over the infinite x-y plane to include the entire beam.

With the probe beam at a position (x', y') during the raster scan, the response of detector $s_\Phi(x', y')$ (A/W) is a measurable quantity determined by

$$s_\Phi(x', y') = \frac{i(x', y')}{P(x', y')}, \tag{3}$$

where $i(x', y')$ is the measured current from the detector. Furthermore, current $i(x', y')$ can be expressed as

$$i(x', y') = \iint_S P(x', y')\Phi_n(x - x', y - y')s(x, y)\mathrm{d}x\mathrm{d}y. \quad (4)$$

From Eq. (4), Eq. (3) becomes

$$s_\Phi(x', y') = \iint_A \Phi_n(x - x', y - y')s(x, y)\mathrm{d}x\mathrm{d}y. \quad (5)$$

The area of the above integral reduces to the area of the irradiance meter's aperture A, since $s(x, y)$ vanishes outside the aperture area. Assuming infinitesimal rastering steps, the integrated response of $s_\Phi(x', y')$ from the detector is

$$\iint_S s_\Phi(x', y')\mathrm{d}x'\mathrm{d}y' = \iint_S \left[\iint_A \Phi_n(x - x', y - y')s(x, y)\mathrm{d}x\mathrm{d}y \right] \mathrm{d}x'\mathrm{d}y'. \quad (6)$$

By changing the order of integration, we have

$$\iint_S s_\Phi(x', y')\mathrm{d}x'\mathrm{d}y' = \iint_A \left[\iint_S \Phi_n(x - x', y - y')\mathrm{d}x'\mathrm{d}y' \right] s(x, y)\mathrm{d}x\mathrm{d}y, \quad (7)$$

or

$$\iint_S s_\Phi(x', y')\mathrm{d}x'\mathrm{d}y' = \iint_A s(x, y)\mathrm{d}x\mathrm{d}y, \quad (8)$$

since the integral of the normalized beam intensity distribution is 1 as defined by Eq. (2). Using Eq. (1), Eq. (8) becomes

$$R = \iint_S s_\Phi(x', y')\mathrm{d}x'\mathrm{d}y', \quad (9)$$

and from Eq. (3) we have

$$R = \iint_S \frac{i(x', y')}{P(x', y')}\mathrm{d}x'\mathrm{d}y'. \quad (10)$$

Note that the spectral irradiance response is independent of the probe beam intensity distribution.

In practice, we scanned the irradiance meter with finite steps and we approximated Eq. (10) with the sum of responses induced by each step as

$$R = \sum_{x',y'} \frac{i(x', y')}{P(x', y')}\Delta x'\Delta y', \quad (11)$$

with a large enough rastering area of the probe beam such that the probe beam induces negligible detector response when it is outside the rastering area. Equation (10) is a good approximation if the step size is small compared with the dimensions of the active area of the irradiance meter, and the spatial response of the meter is reasonably smooth across the active area.

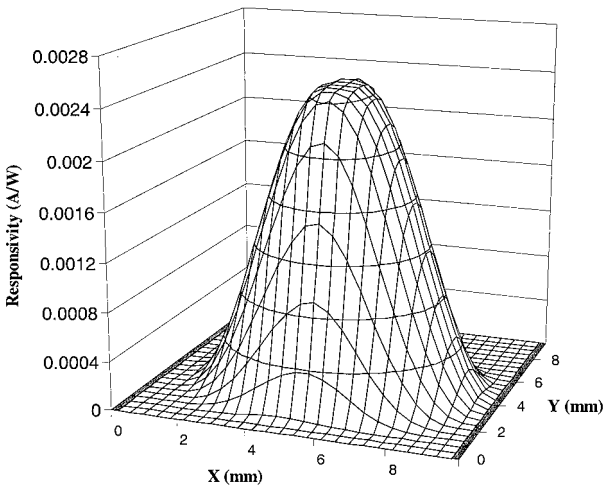

Fig. 2. Measured power responsivity of the irradiance meter by the scanning technique with a 2 mm × 2 mm beam at 157 nm.

4. Irradiance Responsivity Calibration

To determine the irradiance responsivity, the irradiance meter was scanned in the x-y plane inside the test detector chamber, as shown in Fig. 1. The beam size at the detector plane was set to be 2 mm × 2 mm by adjustment of the exit slit of the monochromator. To ensure that the scan of the beam covers the entire active area of the irradiance meter, which is 5 mm in diameter, we scanned the beam in a matrix enclosing an area of 10 mm × 10 mm. The step size was typically 0.4 mm although finer steps were used in some scans to check for measurement accuracy. We measured the irradiance responsivity at three wavelengths, 157, 193, and 320 nm with a 2-nm resolution.

The result of the raster scan at 157 nm is shown in Fig. 2. At the peak of the measured power responsivity, a small plateau of approximately 1-mm dimension indicates the condition of a complete underfill of the beam inside the aperture. The 1-mm dimension is consistent with a 5-mm-diameter aperture scanned by a 2-mm beam.

The responsivity measured outside the central area shows a monotonic decrease when scanning outward, because the probe beam is eclipsed by the aperture and results in a convolution between the beam size and the aperture edge.

Table 1. Irradiance Responsivity of the Irradiance Meter

Wavelength (nm)	Irradiance Responsivity (A cm^2/W)	Central Detector Power Responsivity (A/W)	Effective Area (cm^2)	Physical Area (cm^2)
157	4.879×10^{-4}	2.482×10^{-3}	0.1966	0.1963
193	5.687×10^{-4}	2.900×10^{-3}	0.1961	0.1963
320	1.324×10^{-3}	6.772×10^{-3}	0.1955	0.1963

We calculated the irradiance responsivity of the irradiance meter by summing all the responsivities of the raster scan following Eq. (11). The results are shown in Table 1. Also shown in Table 1 is the power responsivity measured at the center of the irradiance meter and the effective area, or the ratio of the irradiance response and the center responsivity. The measured effective areas are in good agreement with the actual area of the aperture. The fractional differences are less than 0.15% for 157 and 193 nm and 0.4% for 320 nm. This is to be compared with the 0.2% relative uncertainty for the actual area of the aperture. This result validates the scanning technique used for this study and also indicates good spatial uniformity of the photodiode across its active area. The latter was confirmed by a separate measurement of a PtSi photodiode without an aperture in which the uniformity can be scanned for the entire 5-mm-diameter active area of the irradiance meter without being clipped by the aperture. Such good agreement further suggests that irradiance responsivity of the irradiance meter of this study can be derived from the measured central power responsivity of the irradiance meter avoiding the need for raster scanning at each wavelength. Shown in Fig. 3 is the irradiance responsivity of the irradiance meter calculated by the measured power responsivity of the PtSi photodiode and multiplied by aperture area A.

To estimate the uncertainty of the measured irradiance responsivity, we note that the relative uncertainty of the power responsivity is 0.5% (Ref. 5) for the three wavelengths measured by raster scanning. This, combined with the estimated 0.4% relative uncertainty in scanning for aperture area, suggests an estimated relative uncertainty of 0.6% in measured irradiance responsivity.

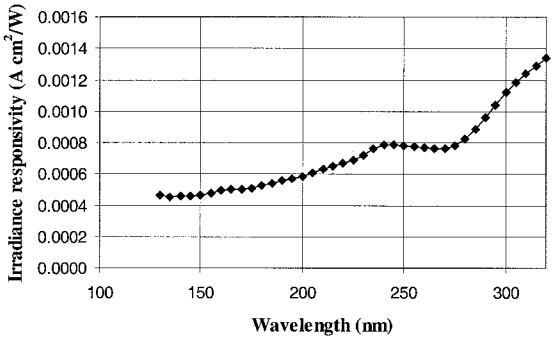

Fig. 3. Irradiance responsivity of the irradiance meter.

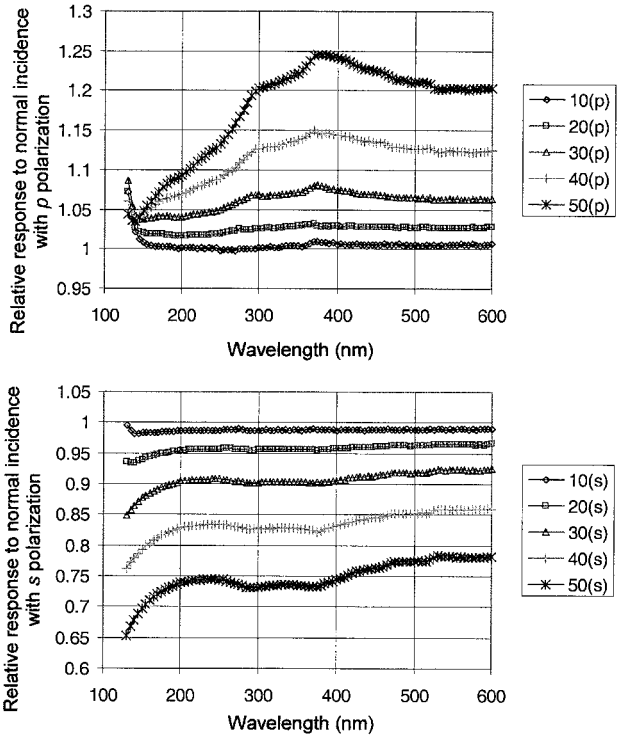

Fig. 4. Angular response of a PtSi photodiode measured at both p polarization and s polarization at 10°, 20°, 30°, 40°, and 50° relative to normal incidence.

The irradiance responsivity of the irradiance meter at the longer wavelengths—around 320 nm—was compared with two other NIST calibration facilities[9]: the Spectral Comparator Facility (SCF) and the SIRCUS Facility. The result from the SCF was in relative agreement with the irradiance responsivity shown in Fig. 3 to within 0.6% around 320 nm. The SIRCUS measurements of irradiance responsivity at 325 nm agreed with the SCF results to within 0.2%. Note that all the measurements discussed above were performed with radiant power well below the saturation region of the photodiode to avoid nonlinear response from the photodiode.

5. Angular Response

Ideally, a cosine response from the irradiance meter is followed when the incident angle of the incoming radiation is changed. This implies that any reflectance from the irradiance meter has to be a constant independent of the incident angle. However, in the case of our instrument, the reflection loss is a function of the angle of incidence and the polarization state determined by the optical properties of the PtSi window and the substrate silicon. Measuring the spectral reflectance at different angles and polarization states provides a direct assessment of the deviation from an ideal cosine response.

We studied the angular response of the irradiance meter by measuring the spectral response of a PtSi

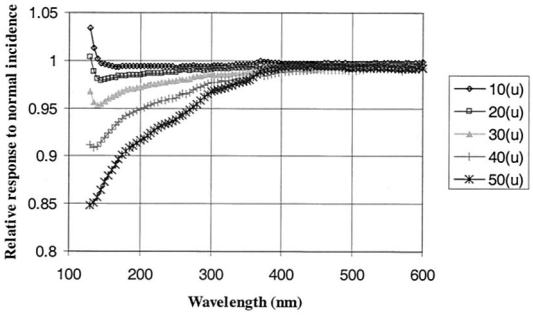

Fig. 5. Angular response of a PtSi photodiode with unpolarized radiation at 10°, 20°, 30°, 40°, and 50° relative to normal incidence.

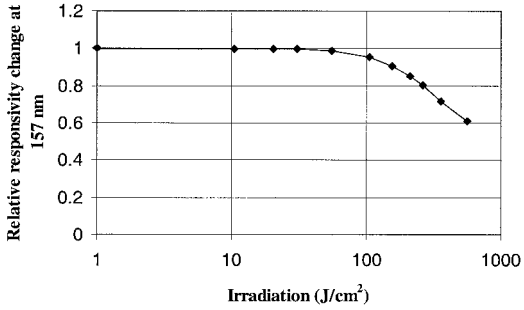

Fig. 6. Degradation of the PtSi photodiode response (at 157 nm) caused by 157-nm excimer laser radiation.

photodiode as a function of incident angle up to 50°. In addition, synchrotron radiation is highly polarized, enabling the angular response for both polarization states to be measured. Figure 4 shows the results of this measurement for both *p* polarization and *s* polarization. At an incident angle of 30°, the relative response is increased by up to 7% for *p* polarization whereas the relative response is decreased by up to 12% for *s* polarization for the spectral range between 157 and 320 nm.

For most industrial applications, the sources, such as discharge lamps or excimer lasers, typically have little or no degree of polarization. Shown in Fig. 5 is the result for unpolarized radiation. Here, the response is decreased by less than 4% at an incident angle of 30° for the spectral range between 157 and 320 nm. Radiation with an incident angle of 30° is at the edge of a solid angle subtended by a numerical aperture of 0.5. Such a large solid angle is often used in commercial photolithography instruments. Poor angular response of an irradiance meter from the ideal cosine response can lead to large uncertainties in measured irradiances. To estimate the uncertainty caused by the angular response of the irradiance meter under study, we assume a uniform irradiation over the solid angle subtended by a numerical aperture of 0.5. In this case, the readings of the irradiance meter decrease by only 2% relative to normal incidence.

Finally, it is of interest to note the excellent angular response from 300 nm to the visible as shown in Fig. 5. In most of the visible, there is a less than 2% change in relative response for incident angles as large as 50°.

6. Radiation Damage

It was shown previously that typical silicon photodiodes exhibit damage effects when exposed to radiation at wavelengths below 250 nm.[12] The damage effects become drastically more pronounced with higher irradiation and at shorter wavelengths. To demonstrate the radiation damage resistance of our irradiance meter, we used a 157-nm excimer laser to induce damage to the photodiode.[13] The excimer laser delivers approximately 1 mJ/cm^2/pulse to the detector with a maximum repetition rate of 100 Hz. Our procedure for this study was as follows: The detector was placed in the test chamber with the monochromator tuned to 157 nm and the response of the detector was measured. We note that the typical power at 157 nm from the monochromator was less than 1 μW, which caused negligible damage to the PtSi photodiode used in this work. Afterward, the photodiode was irradiated with a fixed dose of 157 nm by the excimer laser. Following laser irradiation, the low-power radiation of 157 nm from the monochromator was applied to remeasure the photodiode response. We repeated this cycle until we observed a significant change in the photodiode response.

The measured change of the PtSi photodiode response at 157 nm as a function of irradiation is shown in Fig. 6. No noticeable change in 157-nm responsivity was observed until approximately 100 J/cm^2, which is significantly better than the performance of typical silicon photodiodes[4] although at the expense of much lower responsivity.[4]

For longer wavelengths, such as 193 nm, much higher irradiation is required to reach the damage threshold.[13] Our study at 157 nm provides a limiting case for the PtSi photodiode used as the irradiance meter for this study.

7. Conclusion and Future Studies

A simple irradiance meter was constructed and characterized by use of a cryogenic radiometer-based beamline coupled with synchrotron radiation from the SURF. The irradiance responsivity of the meter was measured from the UV to the VUV by use of the aperture scanning technique. The irradiance meter exhibited reasonable radiation resistance as we demonstrated by using a 157-nm excimer laser. Although the meter does not include a diffuser to improve the angular response, we found an excellent angular response that is well suited for applications such as photolithography for which the typical numerical aperture is 0.5. This meter can be used for many other industrial and environmental applications in the UV and the VUV.

We are in the process of testing more state-of-the-art photodiodes for use in irradiance measurements. Even though the irradiance meter in this study is a broadband detector, it is possible to incorporate filter

devices. Furthermore, it is also possible to modify the PtSi window of the photodiode by altering its thickness or chemical composition to tailor the irradiance responsivity, angular response, and radiation damage for specific applications.

The authors thank Steven W. Brown, George P. Eppeldauer, and Thomas C. Larason for their helpful discussions and suggestions.

References and Notes

1. G. Xu and X. Huang, "Characterization and calibration of broadband ultraviolet radiometers," Metrologia **37,** 235–242 (2000).
2. T. C. Larason and C. L. Cromer, "Sources of error in UV radiation measurements," J. Res. Natl. Inst. Stand. Technol. **106,** 649–656 (2001).
3. R. A. Bosch, D. E. Eisert, M. L. Furst, R. M. Graves, L. Greenler, A. Hamilton, L. R. Hughey, R. P. Madden, P. Robl, P. S. Shaw, W. S. Trzeciak, R. E. Vest, and D. Wahl, "SURF III: A new electron storage ring at NIST," in *Synchrotron Radiation Instrumentation: SRI 99: Eleventh US National Conference*, P. Pianetta, J. Arthur, and S. Brennan, eds., AIP Conf. Proc. **521,** 383–390 (1999).
4. P. S. Shaw, K. R. Lykke, R. Gupta, T. R. O'Brian, U. Arp, H. H. White, T. B. Lucatorto, J. L. Dehmer, and A. C. Parr, "Ultraviolet radiometry with synchrotron radiation and cryogenic radiometry," Appl. Opt. **38,** 18–28 (1999).
5. P. S. Shaw, T. C. Larason, R. Gupta, S. W. Brown, R. E. Vest, and K. R. Lykke, "The new ultraviolet spectral responsivity scale based on cryogenic radiometry at Synchrotron Ultraviolet Radiation Facility III," Rev. Sci. Instrum. **72,** 2242–2247 (2001).
6. S. W. Brown, G. P. Eppeldauer, and K. R. Lykke, "NIST facility for spectral irradiance and radiance responsivity calibrations with uniform sources," Metrologia **37,** 579–582 (2000).
7. J. M. Bridges and C. L. Cromer, "Final report on calibration and characterization of I-line exposure meters," Report 91 090 678A-ENG (International SEMATECH, Austin, Tex., 1991).
8. C. A. Schrama and H. Rejin, "Novel calibration method for filter radiometers," Metrologia **36,** 179–182 (1999).
9. T. C. Larason, S. W. Brown, G. P. Eppeldauer, and K. R. Lykke, "Responsivity calibration methods for 365-nm irradiance meters," IEEE Trans. Instrum. Meas. **50,** 474–477 (2001).
10. Certain commercial equipment, instruments, or materials are identified in this paper to foster understanding. Such identification does not imply recommendation or endorsement by the National Institute of Standards and Technology, nor does it imply that the materials or equipment identified are necessarily the best available for the purpose.
11. K. Solt, H. Melchior, U. Kroth, P. Kuschnerus, V. Persch, H. Rabus, M. Richter, and G. Ulm, "PtSi–*n*–Si Schottky-barrier photodetectors with stable spectral responsivity in the 120–250 nm spectral range," Appl. Phys. Lett. **69,** 3662–3664 (1996).
12. L. Werner, "Ultraviolet stability of silicon photodiodes," Metrologia **35,** 407–411 (1998).
13. P. S. Shaw, T. C. Larason, R. Gupta, and K. R. Lykke, "Characterization of UV detectors at SURF III," Rev. Sci. Instrum. **73,** 1625–1628 (2002).